Design and evaluation of a wasp-inspired steerable needle

Scali, M.; Kreeft (student), Davey; Breedveld, P.; Dodou, D.

DOI
10.1117/12.2259978

Publication date
2017

Document Version
Final published version

Published in
Proceedings Volume 10162, Bioinspiration, Biomimetics, and Bioreplication 2017

Design and evaluation of a wasp-inspired steerable needle

M.Scali[*a], D. Kreeft[a], P. Breedveld[a], D. Dodou[a]
[a] Delft University of Technology, Faculty of Mechanical, Maritime and Materials Engineering, Biomechanical Engineering, Mekelweg 2, Delft, The Netherlands

ABSTRACT

Flexible steerable needles can follow complex curved paths inside the human body. In a previous work, we developed a multiple-part steerable needle prototype with a diameter of 1.2 mm, inspired by the ovipositor of parasitoid wasps. The needle consisted of seven nickel-titanium longitudinally aligned wires held together at the tip by a cylindrical ring with seven holes. The steerability of the needle was evaluated in a gelatin phantom and was found to be lower than that of other steerable needles in the literature. One possible cause of this limited steerability is that during motion the wires tend to separate from each other (i.e., bifurcate). Our aim here was to reduce bifurcation in order to increase the steering curvature of the needle, while keeping the diameter around 1.5 mm, and thus compatible with needles used in medical practice. To achieve that, we changed the shape of the ring from cylindrical to conical. We evaluated the steering performance in gelatin, using the conical ring in two configurations: (1) with the apex of the cone towards the needle tip, so that the wires converge, thus expected to reduce bifurcation, (2) with the apex of the cone placed towards the needle base, so that the wires diverge, thus expected to magnify bifurcation. Results showed that the diverging ring generated larger steering curvatures. We can conclude that reducing the bifurcation of the wires is not enough for increasing the steering curvature and that inducing this same phenomenon instead could actually lead to higher curvatures.

Keywords: Medical needles, steerable needles, biologically inspired design, deflection, steering curvature.

1 INTRODUCTION

In percutaneous interventions, when a target area inside the human body can be reached via a straight line, rigid needles are typically used. However, when the target is difficult to reach and avoiding organs or vessels along the path becomes essential, the physician might decide to proceed with open surgery or to not perform the procedure, with obvious consequences for the patient's health. Over the last decades, researchers have been developing flexible steerable needles (see[1] for a review), which allow to follow complex curved paths. The steering curvature required to reach a target depends on the specific medical procedure. In some cases, such as in brachytherapy, the needle has only to compensate for the movement of tissues and organs in the environment, and so the maximum deviation from a straight path (i.e., deflection) required is relatively small (e.g., between 2 mm and 6 mm).[2] In cases in which the target is blocked by sensitive structures (e.g., vessels), much higher needle deflections are required (e.g., 30 mm) over a relatively short distance from the insertion point (e.g., 80 mm).[3]

1.1 Needle steering curvature

Curvature is a quantitative measure of the amount by which a curve deviates from a straight line. In the case of a circle, the curvature equals the reciprocal of the circle radius at every point. In the case of a general curve, the curvature equals the curvature of the osculating circle, which is the tangent circle that approximates the curve the best. The steerability of a needle is often expressed as the minimum achievable radius of curvature, that is, the reciprocal of the curvature. Alternatively, steerability can be expressed as the ratio of the maximum deviation of the needle from a straight path to the distance between the position from which the needle starts to deflect and the position of maximum deviation,[4] called henceforth 'deflection-to-insertion ratio'. The steering curvature is high when the radius of curvature is low and/or the deflection-to-insertion ratio is high. The steering curvature depends on the needle design characteristics, namely the needle diameter, the type and degree of asymmetry of the needle tip, and the needle material. Decreasing the needle

*m.scali@tudelft.nl: Bio-Inspired Technology Group, www.bitegroup.nl

Bioinspiration, Biomimetics, and Bioreplication 2017, edited by Mato Knez, Akhlesh Lakhtakia, Raúl J. Martín-Palma
Proc. of SPIE Vol. 10162, 1016207 · © 2017 SPIE · CCC code: 0277-786X/17/$18 · doi: 10.1117/12.2259978

diameter lowers the second moment of inertia, resulting in lower bending resistance, thereby increasing the steering curvature.[5] Asymmetry at the needle tip can be induced with a bevel-tip, a pre-bent segment, or a combination of both.[6] The smaller the bevel angle, the higher the curvature. Simulations by Konh et al.[7] indicated that a decrease of the bevel angle from 60° to 20° corresponds to an increase in needle deflection from 7.3 mm to 25.5 mm for an insertion depth of 150 mm and a needle diameter of 0.64 mm. It has further been shown that the effect of the bevel angle on the steering curvature decreases for small bevel angles, with differences in deflection being barely noticeable between needles (Ø1.27 mm) with a bevel angle of 30° and 10°.[8] Asymmetry at the needle tip can be also induced by bending the tip. The bend can be permanent and activated by tissue interaction, or temporary and activated by cables[9] or other means.[10] Increasing the tip angle of a pre-bent needle also increases the steering curvature.[11] Moreover, adding a bend to a conical[3] or bevel-tip needle[12] increases the steering curvature compared to a needle without a bend. Pre-bending bevel-tip needles can considerably improve the steering curvature, with minimum radii of curvature of 16.45 cm versus 5.62 cm reported for bevel-tip versus pre-bent bevel-tip needles, respectively.[6] Another way of lowering the bending resistance of the needle is by carving one or more sets of notches on the needle shaft. In Khadem et al.,[13] adding four sets of notches to a 18G standard needle increased deflection from 25 mm to 33 mm. The steering curvature further depends on the needle material. With stiffness approximately 1/3 of that of standard stainless steel, Nitinol, for example, has been used in needles to increase the steering curvature.[14] Table 1 presents an overview of the minimum radius of curvature and/or maximum needle tip deflection-to-insertion ratio for various needle designs reported in the literature.

1.2 Aim

In previous work,[15] we developed a multiple-part needle prototype inspired by the ovipositor of parasitoid wasps and evaluated its steerability in a gelatin phantom. The needle consists of seven Nitinol wires, each with a diameter of 0.25 mm and a length of 160 mm. Six of the wires are arranged circularly around the seventh wire. An interlocking ring (aluminum, Ø1.2 mm, 2.0 mm long) with seven holes (Ø0.3 mm) keeps the wires together at the tip of the needle. The total diameter of the needle is 1.2 mm at the tip (i.e., equal to the diameter of the ring) and 0.75 mm along the body. The needle is able to advance through a gelatin phantom with zero external push force and to follow a curved path. Specifically, by actuating one or two wires simultaneously, the needle can advance forward within the substrate, as the remaining four or five stationary wires generate sufficient friction force to compensate for the friction and cutting force of the advancing wires. Steering is achieved by creating an offset between adjacent wires, a configuration which we call a 'discrete bevel-tip', and by moving each pair of offset adjacent wires over a pre-defined distance (stroke). Depending on the actuation sequence of the wires, the needle steers to the left or to the right.

We tested several combinations of offset (i.e., 3.6 mm, 1.8 mm, and 0.9 mm) and stroke (i.e., 2 mm, 4 mm, and 6 mm) and found a maximum steering curvature of 0.018 1/cm (average across 5 trials), achieved with an offset of 3.6 mm and a stroke of 2 mm, and a maximum deflection-to-insertion ratio of 0.078 (average across 5 trials), achieved with an offset of 3.6 mm and a stroke of 6 mm. These values are lower than values reported for other needle designs (see Table 1). One possible cause of this limited steerability is that during motion the wires tend to separate from each other (i.e., bifurcate), because of which the discrete bevel loses its definition and the steering motion becomes compromised.

The aim of the present work was to reduce the bifurcation of the wires in order to increase the steering curvature of the needle, while keeping the final diameter smaller than 2 mm, and thus compatible with the diameter of the needles used, for example, in core needle biopsy (14-19G)[16] and brachytherapy (17-18G).[17] We first present the conceptual design of the needle prototype and the steering method used, followed by an experimental evaluation of the steering performance of the needle.

2 NEEDLE DESIGN

2.1 Conceptual design for reducing wire bifurcation

One possible origin of the bifurcation of the wires observed in the previous prototype is the tolerance between the holes of the interlocking ring and the wires (0.025 mm). This space could cause the wires to exhibit play while they move through the holes and to bend towards a direction different from the steering direction. A possible solution could be to increase the length of the interlocking ring, which would limit the bending angle of the wires inside the holes. Accordingly, we increased the length of the interlocking ring of the prototype from 2 mm to 5 mm.

Table 1: State-of-the-art on steering curvatures

Reference	Needle design	Material	Outer diameter [mm]	Smallest radius of curvature [mm]	Deflection-to-insertion ratio [mm/mm]	Insertion speed [mm/s]	Medium
Adebar et al.[3]	Articulated tip (45°, length 9 mm)	Nitinol	0.8 (body), 2.0 (hinge), 1.0 (tip)	82.7	0.42* (27.7/65)	ca. 1.6	Ex vivo porcine liver
Bui et al.[18]	Cannula and stylet with bevel-tip (12°)	Nitinol	0.46 (cannula), 0.24 (stylet)	71.8 265.6 (ex-vivo)	N/A	3	Gelatin 10% Ex-vivo cow liver
Datla et al.[19]	Shape-memory allow (SMA) actuated needle with conical tip	Nitinol (body), stainless steel (tip)	2.20	N/A	0.2* (30/150)	2.55	Plastisol (3:1 ratio plastic to softener)
Khadem et al.[13]	Needle with 4 set of notches	Stainless steel	1.02	198	0.24* (34.29/140)	5	80% liquid plastic and 20% plastic softener (E = 35 kPa)
Ko et al.[20]	Two-segment with bevel-tip	Soft material, Digital Material™ DM_9885 and DM_9895 (body), Rigid material, VeroWhite (tip)	4	ca. 70	N/A	0.5	Gelatin 6% wt (E = 7 kPa)
Ko et al.[21]	Four-segment with bevel tip	Rubber-like material	12	178.6	N/A	1	Gelatin 6% wt (E = 7 kPa)
Konh et al.[7]	Bevel-tip (30°)	Steel	0.38	N/A	0.24* (36/150)	2.5	Plastisol gel (3:1, plastic: softner)
Majewicz et al.[22]	Bevel-tip (30°)	Nitinol	0.58	164.5 (ex vivo)	N/A	5	Kidney (canine)
	Pre-bent (15°) with bevel-tip (30°)	Nitinol	0.58	52.3 (ex vivo) 104 (in vivo)	N/A	5	Kidney (canine)
Majewicz et al.[6]	Pre-bent (45°)	Nitinol	0.58	34	N/A	15	Ex vivo goat liver
Minhas et al.[23]	Pre-bent (15°) with bevel-tip (10°)	Nitinol (body), stainless steel (bevel-tip)	1.27 (tip) 0.28 (body)	52*	N/A		Gelatin 6.5% wt
Misra et al.[24]	Bevel-tip (38°)	Nitinol	0.4	179.4	0.78* (98/125)	2.5	Plastisol (4:1 ratio pastic to softner)
Okazawa et al.[25]	Straight cannula and pre-bent stylet	Nitinol	0.81	N/A	0.35* (35/100)	5	Polyvinyl chloride compound (E = 157 kPa)

Ryu et al.[26]	SMA actuation needle with symmetric tip	Nitinol and PTFE	1.67	N/A	0.12* (7.2/60)	0.5	Plastisol (4:1 ratio plastic to softner, E = 40 kPa)
Rucker et al.[27]	Bevel-tip (35°)	Nitinol	0.86	128 400 (ex vivo)	N/A	N/A	Simulated Muscle Tissue Ballistic Test Media (Sim-Test) Ex vivo bovine liver
Swaney et al.[12]	Bevel-tip (10° bevel angle) with flexure (max angle 22°)	Stainless steel (body), Nitinol (flexure)	0.91	121 (gelatin) 176 (ex vivo)	N/A	5	Gelatin 10% wt Ex vivo pork loin
Patil et al.[14]	Pre-bent with bevel-tip	Nitinol	0.88	67* 137* (ex vivo)	N/A	N/A	Simulated Muscle Tissue Ballistic Test Media (Sim-Test), Corbin, Inc (5:1 ratio with water)
Wellborn et al.[4]	Flexure needle tip, bevel-tip (10°) with notched wall sheath	Nitinol	0.91 (stylet)	N/A	1.1 (gelatin) 0.21 (ex vivo)	N/A	Knox gelatin phantom 10% wt Ex vivo bovine liver
Wood et al.[28]	Bevel-tip (7°)	Nitinol	0.52	333*	N/A	N/A	Kidney phantom (medical training model, Limbs & Things, Inc., Savannah, Ga.)

*The value has been calculated by us based on numerical data given in the original paper. When not provided, the numbers have been extracted from graphs shown in the original paper.
N/A: Information not available.

Bifurcation could be further reduced by guiding the wires towards the central wire. To achieve that, we changed the shape of the interlocking ring from cylindrical to conical. By creating an angle with respect to the longitudinal axis of the needle, the wires would mimic a pre-bent needle, converging towards the central wire. This ring will be henceforth referred to as 'converging ring' (Figure 1). The angle β of the conical ring with respect to the longitudinal axis of the ring can be defined as a function of the minimum and maximum diameter d_1 and d_2 of the ring and its length l:

$$d_2 = 2l \tan\beta + d_1 \tag{1}$$

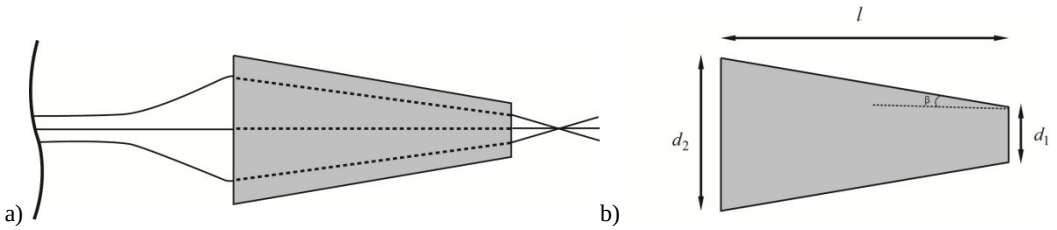

Figure 1. a) Schematic representation of the converging ring with the wires guided towards the center. The vertical curved line on the left indicates the continuation of the needle body towards the needle base. The needle tip is depicted at the rightmost side of the drawing. b) Design parameters of the conical ring. d_1 and d_2 are the minimum and maximum diameters, respectively, l is the length of the ring, and β is the angle with respect to the longitudinal axis of the ring.

Assuming l = 5 mm, d_1 = 1.2 mm, and β = 2°, it can be derived from Eq. (1) that d_2 = 1.55 mm. The total diameter of the prototype coincides with the ring diameter, which is 1.55 mm (i.e., lower than 2 mm).

To test our hypothesis that the bifurcation of the wires was the main cause of limited steering in our previous prototype, we also created a ring that intentionally induces bifurcation of the wires and observed the effect of such a ring on the steering curvature. This ring is identical to the converging ring described above, but with its apex placed towards the base of the needle, so that the wires are moved away from the central wire, therefore magnifying the bifurcation (Figure 2). This ring will be henceforth referred to as 'diverging ring'.

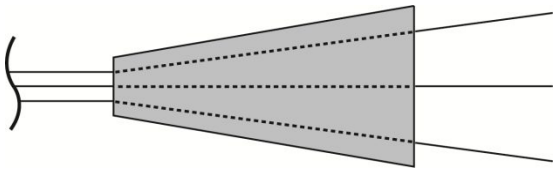

Figure 2. Schematic representation of the diverging ring. The vertical curved line on the left indicates the continuation of the needle body towards the needle base. The needle tip is depicted at the rightmost side of the drawing.

2.2 Needle prototype

The needle prototype consists of a needle body and an actuation unit. The needle body consists of seven longitudinally aligned wires of Nitinol (straight annealed, activation temperature 20°C), each wire with a diameter of 0.25 mm and a length of 250 mm. The wires are held together at the needle tip by the converging/diverging ring described in Section 2.1. The ring has one central 0.3-mm hole and six 0.3-mm circumferential holes through which the wires are fed. The central wire is glued to the central hole, while the other six wires can slide back and forth through the circumferential holes. Six stainless steel rings (Øin: 0.9 mm, Øout: 1.0 mm, 2.0 mm long) are located along the length of the needle, to keep the Nitinol wires together (Figure 3).

The actuation unit consists of six stepper motors AM0820 with step angle 18º (Faulhaber, Germany), each motor actuating one of the six wires. The transmission consists of a leadscrew (M2, 28 mm long) and a slider to convert rotational motion of the stepper motors into a linear motion of the wires. Seven stainless steel tubes are attached to the housing to guide the seven wires outside of the actuation unit. The six stepper motors are actuated using six stepper drivers DRV8834 (Texas Instruments, TX) and an Arduino MEGA 2560 micro-controller.

a) 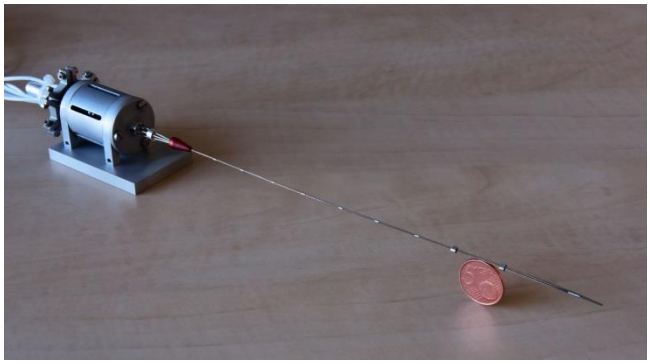 b) 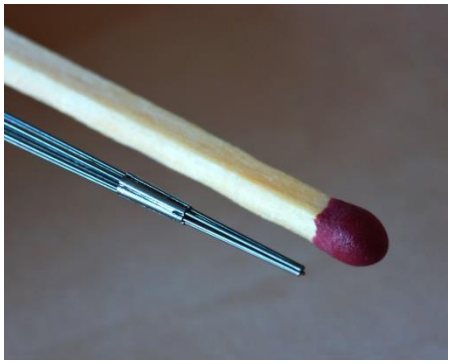

Figure 3. a) Needle prototype with the actuation unit at the leftmost side of the photo. b) Close-up of the needle tip with the converging ring.

2.3 Steering motion

We expect that the steering curvature is higher when using the converging ring as compared to the diverging ring, because in the former case the wires have the tendency to move towards the center, thereby averting bifurcation, whereas

in the latter case the wires are forced to bifurcate and the definition of the discrete bevel-tip is lost. Additionally, in the case of the converging ring, the wires mimic the behavior of pre-bent wires, which increases the lateral forces acting at the end side and is thus expected to result in higher steering curvature.

In order to lay a curved path, first an offset (*O*) is created by moving two pairs of adjacent wire forward, one at the time, while the third pair remains stationary. Then, each of the three pairs is moved forward, one at the time, over a pre-defined distance called stroke (*S*). Because of the asymmetry created at the tip by the offset and stroke, the needle deflects. Finally, all six wires are moved backwards, causing the interlocking mechanism that is glued to the central wire to advance within the substrate. By repeating these steps, the needle follows a curved path inside the substrate. Depending on the desired steering direction (left or right) different pairs of wires are actuated. Steering to the left is achieved by moving over a pre-defined *O* the wire pairs 1-2 and 3-4 for the converging ring and 1-6 and 5-4 for the diverging ring. For steering to the right, wire pairs 1-6 and 5-4 are moved for the converging ring and 1-2 and 3-4 for the diverging ring (Figure 4).

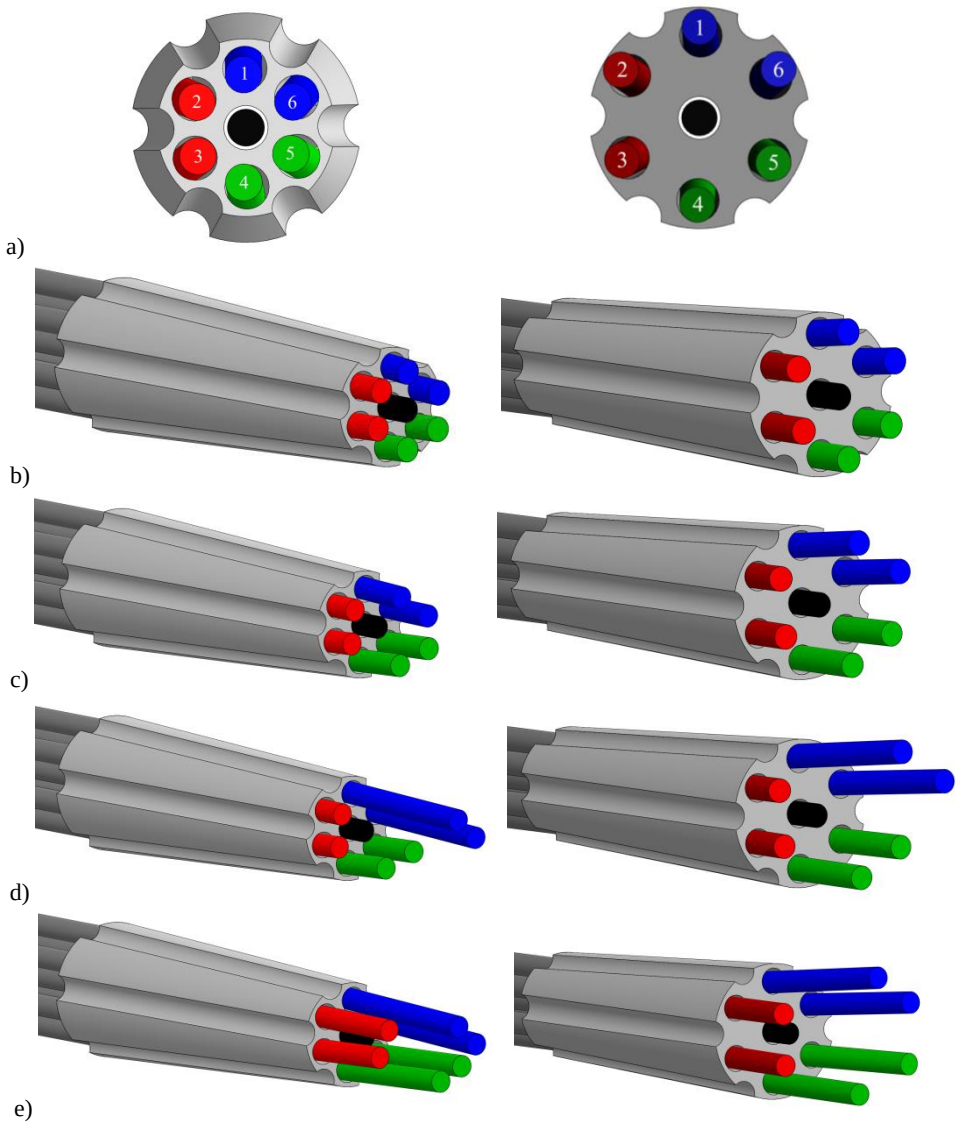

Figure 4. The steps of the actuation of the wires used for steering the needle through a substrate with the converging tip (left) and the diverging tip (right). a) Cross-section of the rings, b) Initial position of the wires, c) An offset (*O*) is created by moving two pairs of wires forward over a pre-defined distance called offset (*O*), d) The first pair of wires is moved over a second pre-defined distance, called stroke (*S*), e) The other pairs are moved over the same distance *S*.

3 MATERIALS AND METHODS

The steerability of the two variations of the prototype (i.e., with the converging and the diverging ring) was experimentally evaluated in a gelatin phantom.

3.1 Experimental setup

The experimental setup consisted of an actuation unit mounted on an aluminum platform and data acquisition systems. The base plate of the platform (ca. 405 x 101 mm) had a duct to guide a lightweight aluminum cross-shaped cart (dimensions: 210 x 100 mm, mass = 39 g) mounted to four wheels in order to move along a straight path with low friction. The cart was used to carry a gelatin phantom, in which the needle was inserted (Figure 5). To align the needle along its length, we added two rings with an asymmetric cross-section (aluminum, Ø 3.0 mm, 2.0 mm long) to the body of the needle and fixed them to the cart. The alignment rings had seven holes through which the wires could freely slide. A camera (Nikon D610 with AF-S NIKKOR 24-70 mm) was positioned above the cart to take a photo of the initial insertion and final position of the needle during the trials.

The gelatin phantoms were prepared by mixing hot tap water (ca. 70°C) and gelatin powder (Dr. Oetker Professional, The Netherlands). The solution was poured into containers (ca. 230 x 150 x 60 mm) and stored overnight at 5°C. Before each trial, a gelatin block of 48 x 165 x 30 mm (width x length x height, 200.0 ± 0.2 g) was cut and placed on the cart. The gelatin phantoms had a concentration of 5% weight (wt) powder in water, corresponding to a stiffness of 4.6 kPa, which was measured using an universal testing machine (Zwick/Roell Z005, Germany). This value roughly corresponds to the stiffness of brain tissue (0.5-6.0 kPa)[29]. For all experimental trials, we selected a constant forward speed of 1 mm/s and a theoretical travel distance equal to 120 mm.

a)

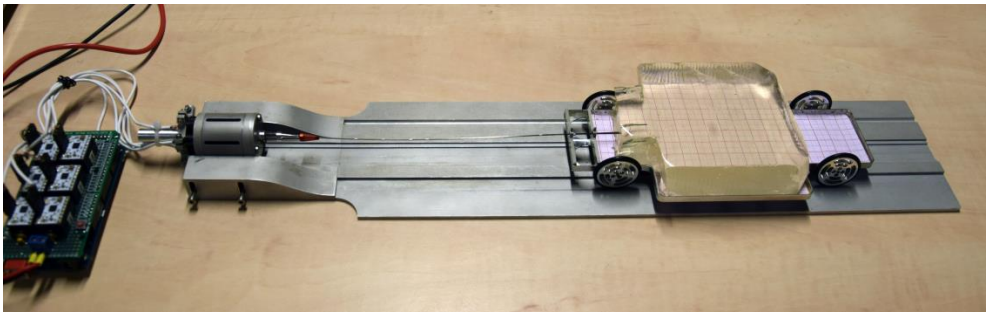

b)

Figure 5. a) Experimental setup showing the actuation unit mounted on an aluminum platform and the gelatin phantom on the cart. b) Close-up of the needle entering the gelatin.

3.2 Experimental design

Hypotheses: Three hypotheses were formulated: a) The higher the offset of the wires, the higher the curvature achieved (i.e., lower radius of curvature), as the asymmetry at the tip increases, causing the needle to bend more. b) The higher the stroke, the higher the curvature achieved (i.e., lower radius of curvature), as the asymmetry at the tip increases, causing the needle to bend more. c) The converging ring reduces the bifurcation of the wires, resulting in higher curvatures than the diverging ring.

Dependent and independent variables: The dependent variable was the deflection-to-insertion ratio of the needle. The independent variables were the initial offset (*O*) of the wires, the stroke (*S*), the steering direction, and the type of ring. The offset was varied between 2.0, 4.0, and 6.0 mm. The stroke was varied between 4.0 and 6.0 mm. Two steering directions, left and right, were tested, and two interlocking rings, converging and diverging. Table 2 shows the eight experimental conditions tested for each interlocking ring.

Table 2. Experimental conditions for each of the interlocking rings.

Condition	Offset [mm]	Stroke [mm]	Direction
1	4.0	4.0	Left
2	6.0	4.0	Left
3	2.0	6.0	Left
4	6.0	6.0	Left
5	4.0	4.0	Right
6	6.0	4.0	Right
7	2.0	6.0	Right
8	6.0	6.0	Right

Experimental procedure: All eight conditions were repeated eight times in a randomized order, first with the converging ring and then with diverging ring. With the help of the actuation unit, the needle was inserted inside the gelatin to a starting position of approximately 35 mm when using the converging ring, and of 45 mm when using the diverging ring; the initial insertion depth was smaller for the converging ring because this ring had a lower drag than the diverging ring. Once the needle was in place, the chosen settings for steering (i.e., *O*, *S*, and direction) were uploaded in Arduino and used for the actuation of the wires. At the end of each trial a photo of the final position was taken, the gelatin was removed from the cart, and the wires were cleaned with oil and water. Measurements that were not successful due to, for example, a failure of the motors, were repeated following a randomized order.

Data analysis: The photographs of the final position of the needle inside the gelatin were cropped to exclude the initial insertion of 35 mm and 45 mm for the converging and the diverging ring, respectively. Then, the MATLAB image processing toolbox was used to convert the photographs into binary images, after which the needle shape and centerline were extracted. Next, the initial and end points were extracted and used to calculate the deflection *d* of the needle from a straight path and the insertion depth *i* (Figure 6). The deflection-to-insertion ratio *d*/*i* was then calculated as a measure of needle curvature.

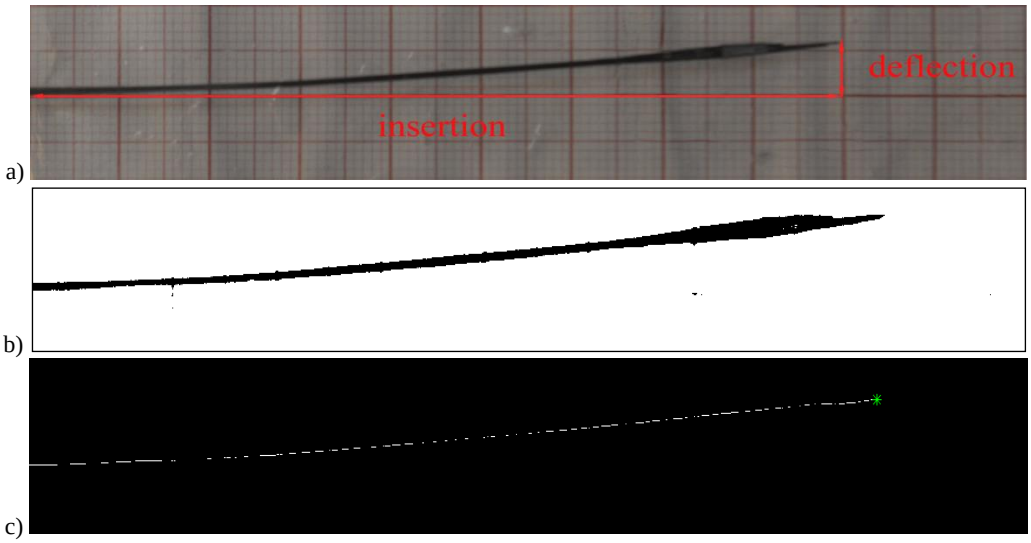

Figure 6. Image processing of experimental data. a) Original image of the final position of the needle. b) Binary image. c) Skeleton with end points. This image corresponds to a measurement for Condition 2 (offset 6 mm, stroke 4 mm, left) with the converging ring.

4 RESULTS

4.1 Converging ring

The measurements for the converging interlocking ring were initially completed successfully 61 out of 64 times. The three failed measurements were caused by motors not actuating the wires correctly and were repeated. The needle steered to a direction opposite to the one expected two times in Condition 6 and two times in Condition 8; these four measurements were excluded from the analysis. Another three measurements (one measurement for each of Conditions 4, 5, and 6) were excluded, because the needle touched the bottom of the cart. The results are summarized in Table 3 and Figure 7. The highest mean deflection-to-insertion depth ratio was 0.069, achieved for Condition 4 (i.e., offset 6 mm, stroke 6 mm, and direction left), with a standard deviation of 0.027. Among the conditions with high deflection-to-insertion ratio (i.e., > 0.050), Condition 1 showed the lowest variability (i.e., standard deviation of 0.019).

4.2 Diverging ring

The measurements for the diverging ring were initially completed successfully 55 out of 64 times. The nine failed measurements were caused by motors not actuating the wires correctly and were repeated. The needle steered in a direction opposite to the one expected in one measurement for Condition 2 and in one measurement for Condition 4; these measurements were excluded from the analysis. The results are summarized in Table 3 and Figure 7. Condition 7 exhibited the highest mean deflection-to-insertion ratio: 0.097, with standard deviation of 0.033. Steering to the right led to higher deflection-to-insertion ratios than steering to the left.

Table 3: Results for steering with the converging ring and the diverging ring

Condition	**Converging ring**		**Diverging ring**	
	Sample size	Deflection-to-insertion ratio (mean ± standard deviation)	Sample size	Deflection-to-insertion ratio (mean ± standard deviation)
1 (O4-S4-L)	8	0.065 ± 0.019	8	0.054 ± 0.034
2 (O6-S4-L)	8	0.063 ± 0.033	7	0.060 ± 0.022
3 (O2-S6-L)	8	0.047 ± 0.022	8	0.054 ± 0.029
4 (O6-S6-L)	7	0.069 ± 0.027	7	0.080 ± 0.042
5 (O4-S4-R)	7	0.033 ± 0.019	8	0.093 ± 0.022
6 (O6-S4-R)	5	0.048 ± 0.024	8	0.096 ± 0.025
7 (O2-S6-R)	8	0.019 ± 0.013	8	0.097 ± 0.033
8 (O6-S6-R)	6	0.049 ± 0.033	8	0.094 ± 0.059

For the same steering direction (left or right), no significant differences in the deflection-to-insertion ratio were found between any of the offset or stroke conditions for either interlocking mechanism. For the converging ring, steering to the left resulted in a significantly higher deflection-to-insertion ratio than steering to the right for Conditions 3 (Mann-Whitney $U = 7$, $p = 0.007$, $r = 0.65$) and 4 ($U = 7$, $p = 0.026$, $r = 0.60$). For the diverging ring, steering to the right resulted in a significantly higher deflection-to-insertion ratio than steering to the left for Conditions 6 ($U = 9$, $p = 0.029$, $r = 0.57$) and 7 ($U = 9$, $p = 0.015$, $r = 0.60$). The diverging ring led to significantly larger curvatures than the converging ring in Conditions 5 ($U = 1$, $p = 0.001$, $r = 0.80$), 6 ($U= 3$, $p = 0.011$, $r = 0.69$), and 7 ($U = 0$, p = 0.00016, $r = 0.84$).

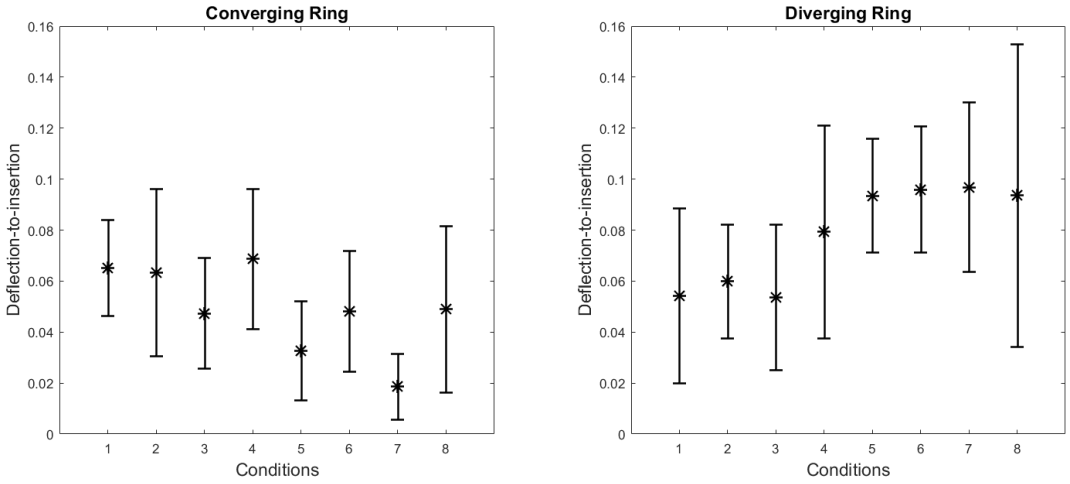

Figure 7. Deflection-to-insertion ratio when using the converging ring and diverging ring. The asterisk represents the mean value and the error bars represent the standard deviation.

5 DISCUSSION

In this study we have presented a prototype of an ovipositor-inspired needle composed of seven Nitinol wires kept together at the needle tip with a conical interlocking ring. Our goal was to prevent the bifurcation of the wires, a phenomenon observed in a previous version of the prototype,[15] and consequently to increase the steering curvature. The conical ring was used in two different configurations: (1) as a 'converging ring', where the wires tend to move toward the center, (2) as a 'diverging ring', where the wires tend to move away from the center. The performance of the needle with both rings has been investigated in a 5%wt gelatin phantom.

In a previous version of the prototype[15] we were creating first an asymmetry between two wires and then reinforcing it by advancing two other wires with the same offset. In the current prototype the offset is created between four wires (i.e., two pairs) and the other two wires (i.e., one pair). The goal of the asymmetry in the first prototype was to create a 'discrete bevel tip' which would then make the needle curve in the direction of the bevel. In the current prototype, we use the offset and the stroke to create an asymmetry that mimics a pre-bent tip. Using a pre-bent tip allows for higher curvatures than a normal bevel-tip needle (see Section 1.1).

The results showed that for three out of the eight tested conditions (Conditions 5, 6, and 7), the diverging ring led to statistically higher steering curvatures than the converging ring, which is against our hypothesis. A possible reason why the converging ring led to lower steering curvatures than the diverging ring is the interaction between the wires, which is present when using the converging ring and not with the diverging ring. Specifically, during the actuation sequence, some of the wires are protruding because of the offset created between them (see Figure 4c). When the wires are moved over a distance equal to the stroke, the pair of wires that lies behind pushes the protruded wires towards the opposite direction, reducing the final curvature. Another possible explanation for the unexpected steering performance of the diverging ring is the following: with the converging ring, the wires are directed first outwards when entering the holes, and then inwards when exiting the holes, as the diameter of the ring decreases over the ring length (Figure 1a). With the diverging ring, on the other hand, the wires are directed only outwards. In other words, in the converging ring the wires are bent twice, whereas in the diverging ring, they are bent only once. This might have affected their local stiffness, which could explain why the steering curvatures obtained with the converging ring were smaller than the curvatures obtained with the diverging ring.

In the previous prototype, the steering direction was opposite to the expected one (i.e., needle steering to the left while it was expected to steer to the right and vice versa) in 8 out of 50 trials (16%), whereas in the current prototype, this phenomenon was observed in 6 out of 128 trials (4.69%; 2 of which with the diverging ring). The reduced incidences of 'wrong' steering could be explained by the fact that, whereas the tolerance of the interlocking ring in the previous

prototype made the wires occasionally follow random directions, in the current prototype the motion of the wires was better controllable and therefore the final direction was more predictable.

The highest mean value (0.097, Condition 7) of deflection-to-insertion ratio obtained with the diverging ring is comparable to those reported by Ryu et al.,[25] that is, 0.12 for a needle diameter of 1.67 mm. The ratio corresponds to deflections of around 10 mm over a distance of 90 mm. Such a needle can be used to compensate for motion of tissues and organs in the environment and/or the targets in brachytherapy.[2]

The total length of the offset and stroke created between the wires can be seen as the length of a pre-bent segment. Adebar et al.[3] showed that an increase in the length of the bent-tip leads to higher curvatures. In our case the values of this length (i.e., offset + stroke) are 8, 10, and 12 mm (see Table 2). With the converging ring, the deflection-to-insertion ratio is indeed higher when the sum of the offset and stroke is higher (i.e., 6 + 6 = 12 mm); this difference is less visible for the diverging ring. The reason of this might be that with the diverging ring the wires need just a small offset to bend, and the effect of the additional stroke does not change the amount of steering; moreover, the wires in the case of the diverging ring are already pre-directed towards a certain direction (i.e., controllably bifurcated), and since there is no interaction between the wires, the offset might not be contributing to steering.

One limitation of this work was that the transmissions of individual wires occasionally jammed and the motors got stuck. A different design of the housing of the motors could solve this problem. For example, a larger actuation unit could be used, where the motors with their relative spindles are not constrained, so that they do not get stuck against the wall of the case. Second, we observed that the deflection-to-insertion ratio differed between the two steering direction, left and right. Specifically, the needle steered more to the right than to the left in the case of the diverging ring, and vice versa in the case of the converging ring. This could have been caused by a bias in the wires or by an axial rotation of the ring, making the wires twist, thereby affecting their movement and bending curvature. Third, during our tests we have assumed that the needle deflection occurs only in the steering plane. However, during the experiments we observed that the needle also tended to deflect downwards. This phenomenon is likely to have been caused by the weight of the interlocking ring. Jahya et al.[30] also reported such an 'out of plane' deflection and showed that this phenomenon increases with the degree of bevel angle. Fourth, real-time control of the motors actuation was not possible, since the settings were chosen and loaded every time before the start of each test. A continuous instead of stepwise motion would be preferred, in order to limit any effects of the inertia of the gelatin cart on the motion of the needle.

In future work, the steering curvature of the ovipositor-inspired needle can be increased by decreasing the diameter of the needle.[5] This can be done by using fewer wires and/or wires with a smaller diameter. The wires can also be treated, in order to create a fixed asymmetry at the tip; for example, heat treatment can be used to curve the distal end.[31] A flexible or compliant structure to keep the wires together instead of a rigid interlocking ring could also assist in increasing steerability. Finally, the needle should be tested in substrates with different degrees of stiffness and heterogeneity.

6 CONCLUSION

This paper presents a design solution to increase the steering curvature of a wasp ovipositor-inspired needle with a diameter of 1.55 mm. We showed that the needle can steer through a 5%wt gelatin phantom by generating an asymmetry at the tip and two configurations of a conical interlocking mechanism (converging and diverging) that mimics a pre-bent needle. The highest mean deflection-to-insertion ratio achieved was 0.097 (standard deviation of 0.033), which is higher than the corresponding ratio of 0.078 achieved by a previous version of the prototype with a straight interlocking ring. This higher ratio was achieved, however, when using the diverging rather than the converging conical ring, which runs opposite to our hypothesis. We can conclude that reducing the bifurcation of the wires is not enough for increasing the steering curvature and that inducing this same phenomenon instead could lead to higher curvatures.

7 ACKNOWLEDGMENT

This research is supported by the Netherlands Organisation for Scientific Research (NWO), domain Applied and Engineering Sciences (TTW), and which is partly funded by the Ministry of Economic Affairs (project number 12712, iMIT-Instruments for Minimally Invasive Techniques). The authors would like to thank Menno Lageweg and Danny de Gans from the Central Workshop (DEMO) of the TU Delft for their design advice and needle prototype manufacturing.

REFERENCES

[1] Scali, M., Pusch, T. P., Breedveld, P. and Dodou, D., "Needle-like instruments for steering through solid organs: A review of the scientific and patent literature," Proc. Inst. Mech. Eng. H: J. Eng. Med. 231(3), 250-265 (2016).

[2] Stone, N. N., Roy, J., Hong, S., Lo, Y.C. and Stock, R.G., "Prostate gland motion and deformation caused by needle placement during brachytherapy," Brachytherapy 1(3), 154-160 (2002).

[3] Adebar, T. K., Greer, J. D., Laeseke, P. F., Hwang, G. L. and Okamura, A. M., "Methods for improving the curvature of steerable needles in biological tissue," IEEE Trans. Biomed. Eng. 63(6), 1167-1177 (2016).

[4] Wellborn, P.S., Swaney, P. J. and Webster, R. J., "Curving clinical biopsy needles: can we steer needles and still obtain core biopsy samples?," J. Med. Devices 10(3), 030904 (2016).

[5] van Veen, Y. R., Jahya, A. and Misra, S., "Macroscopic and microscopic observations of needle insertion into gels," Proc. Inst. Mech. Eng. H: J. Eng. Med. 226(6), 441-449 (2012).

[6] Majewicz, A., Wedlick, T. R., Reed, K., B. and Okamura, A. M., "Evaluation of robotic needle steering in ex vivo tissue," Proc. IEEE Int. Conf. Robotics and Automation, 2068-2073 (2010).

[7] Konh, B., Honarvar, M., Darvish, K. and Hutapea, P., "Simulation and experimental studies in needle-tissue interactions," J. Clin. Monit. Comput. 18, 1-2 (2016).

[8] Jiang, S. and Wang, X., "Mechanics-based interactive modeling for medical flexible needle insertion in consideration of nonlinear factors," J. Comput. Nonlin. Dyn. 11(1), 011004 (2016).

[9] van de Berg, N. J., Dankelman, J. and van den Dobbelsteen, J. J., "Design of an actively controlled steerable needle with tendon actuation and FBG-based shape sensing," Med. Eng. Phys. 37(6), 617-622 (2015).

[10] Ayvali, E., Ho, M. and Desai, J. P., "A novel discretely actuated steerable probe for percutaneous procedures," In Experimental Robotics, Springer, 115-123 (2014).

[11] Wedlick, T. R and Okamura, A. M., "Characterization of pre-curved needles for steering in tissue," Proc. IEEE Eng. Med. Biol. Soc., 1200–1203 (2009).

[12] Swaney, P. J., Burgner, J., Gilbert, H. B. and Webster, R. J., "A flexure-based steerable needle: high curvature with reduced tissue damage," IEEE Trans. Biom. Eng. 60(4), 906-909 (2013).

[13] Khadem, M., Rossa, C., Usmani, N, Sloboda, R. S. and Tavakoli, M., "Introducing notched flexible needles with increased deflection curvature in soft tissue," IEEE Int. Conf. on Advanced Intelligent Mechatronics (AIM), 1186-1191 (2016).

[14] Patil, S., Burgner J, Webster RJ, Alterovitz R., "Needle steering in 3-D via rapid replanning," IEEE Trans. Rob. 30(4), 853-864 (2014).

[15] Scali, M., Pusch, T. P., Breedveld, P. and Dodou, D., "Ovipositor-inspired steerable needle: design and preliminary experimental evaluation," Manuscript submitted (2017).

[16] Gherardi, G., [Fine-needle Biopsy of Superficial and Deep Masses: Interventional Approach and Interpretation Methodology by Pattern Recognition] Springer Science & Business Media (2010).

[17] Podder, T., Clark, D., Sherman, J., Fuller, D., Messing, E., Rubens, D., Strang, J., Brasacchio, R., Liao, L., Ng, W. S. and Yu, Y., "In vivo motion and force measurement of surgical needle intervention during prostate brachytherapy," Med. Phys. 33(8), 2915-2922 (2006).

[18] Bui, V. K., Sukho P., Park, J. O. and Ko, S. Y., "A novel curvature-controllable steerable needle for percutaneous intervention," Proc. Inst. Mech. Eng. H: J. Eng. Med. 230(8), 727-738 (2016).

[19] Datla, N. V., Konh, B. and Hutapea, P., "Studies with SMA actuated needle for steering within tissue," ASME Conf. on Smart Material Adaptive Structures and Intelligent Systems (SMASIS), (2014).

[20] Ko, S. Y. and y Baena, F. R., "Toward a miniaturized needle steering system with path planning for obstacle avoidance," IEEE Trans. Biom. Eng. 60(4), 910-7 (2013).

[21] Ko, S. Y., Frasson, L., and y Baena, F. R., "Closed-loop planar motion control of a steerable probe with a "programmable bevel" inspired by nature," IEEE Trans. Robot. 27(5), 970-83 (2011).

[22] Majewicz, A., Marra, S. P., van Vledder, M. G., Lin, M., Choti, M. A., Song, D. Y. and Okamura, A. M., "Behavior of tip-steerable needles in ex vivo and in vivo tissue," IEEE Trans. Biomed. Eng. 59(10), 2705-15 (2012).

[23] Minhas, D. S., Engh, J. A., Fenske, M. M., Riviere, C. N., "Modeling of needle steering via duty-cycled spinning," Proc. IEEE Eng. Med. Biol. Soc. 29th Annu. Int. Conf., 2756-59 (2007).

[24] Misra, S., Reed, K. B., Schafer, B. W., Ramesh, K. T. and Okamura A. M., "Observations and models for needle-tissue interactions," IEEE Int. Conf. Robot. Autom., 2687-92 (2009).

[25] Okazawa, S., Ebrahimi, R., Chuang, J., Salcudean, S. E. and Rohling, R., "Hand-held steerable needle device," IEEE/ASME Trans. Mechatron. 10(3), 285-96 (2005).
[26] Ryu, S. C., Quek, Z. F., Koh, J. S., Renaud, P., Black, R. J., Moslehi, B., Daniel, B. L., Cho, K. J. and Cutkosky, M. R., "Design of an optically controlled MR-compatible active needle," IEEE Trans. Robot. 31(1), 1-11 (2015).
[27] Rucker, D. C., Das, J., Gilbert, H. B., Swaney, P. J., Miga, M. I., Sarkar, N. and Webster, R. J., "Sliding mode control of steerable needles," IEEE Trans. Robot. 29(5), 1289-99 (2013).
[28] Wood, N. A., Shahrour, K., Ost, M. C. and Riviere, C. N., "Needle steering system using duty-cycled rotation for percutaneous kidney access," Proc. IEEE Eng. Med. Biol. Soc. Int. Conf., 5432-35 (2010).
[29] Farrer, A. I., Odéen, H., de Bever, J., Coats, B., Parker, D. L., Payne, A. and Christensen, D. A., "Characterization and evaluation of tissue-mimicking gelatin phantoms for use with MRgFUS," J. Ther. Ultrasound 3(9), (2015).
[30] Jahya, A., van der Heijden, F. and Misra, S., "Observations of three-dimensional needle deflection during insertion into soft tissue," Proc. IEEE/EMBS Int. Conf. Biomed. Robot. Biomechatron., 1205-10 (2012).
[31] Gilbert, H. B. and Webster, R. J., "Rapid, reliable shape setting of superelastic nitinol for prototyping robots," IEEE Robot. Autom. Lett. 1(1), 98-105 (2016).